CRYSTAL GROWTH & DESIGN
2008
VOL. 8, NO. 8
2748–2752

Trapeziform Ag Nanosheet Arrays Induced by Electrochemical Deposition on Au-Coated Substrate

Guangqiang Liu, Weiping Cai,* and Changhao Liang

Key Laboratory of Materials Physics, Anhui Key Laboratory of Nanomaterials and Nanotechnology, Institute of Solid State Physics, Chinese Academy of Sciences, Hefei 230031, P. R. China

Received September 25, 2007; Revised Manuscript Received April 28, 2008

ABSTRACT: Trapeziform Ag nanoplate arrays are successfully fabricated on Au-coated silicon substrate by electrochemical deposition. The trapeziform Ag nanoplates are standing on the substrate and dispersed uniformly. The nanoplates are 1−2 μm in edge length and 40 nm in thickness. Further experiments have revealed that the presence of PVP in the electrolyte and low deposition current density together with the Au-coated substrate are indispensable to fabrication of such arrays. The formation of trapeziform Ag nanoplate arrays is attributed to selectively oriented nucleation of Ag and quasi-equilibrium preferential growth on the Au film-coated substrate. This study is of importance in vertical immobilization Ag nanoplates on a solid substrate, which could provide new substrates for some catalysis or surface-enhanced Raman scattering.

1. Introduction

It has been demonstrated that the intrinsic properties of nanostructured metals can be tailored by controlling their size, composition, and especially, shape.[1–4] The nanostructured metals, especially, noble metals, have attracted much attention in recent years because of their unique properties and hence potential applications in optics,[5] optoelectronics,[6] imaging,[7] information storage,[8] catalysis,[9] biological,[10] chemical sensing,[11] and surface-enhanced Raman scattering (SERS). [12] For instance, the field-enhancement effect near the triangle tips of a metal nanoplate makes it have important applications in atomic force microscopy (AFM), scanning tunneling microscope (STM), and scanning near-field optical microscopy (SNOM).[13] Ag nanoplates, because of their size- and shape-sensitive surface plasmon resonance bands, are regarded as an effective substrate for diagnosis. Up to now, a variety of methods have been developed to prepare Ag nanoplates.[14] Mirkin et al. reported a light-induced approach to transform small silver nanoparticles into nanoprisms with the help of citrate and a coligand such as bis(*p*-sulfonatophenyl)phenylphosphine dehydtate dipotassium.[15] Xia et al. introduced a new and versatile method for the kinetically controlled synthesis of Ag triangular nanoplates.[16] Chen and Carroll demonstrated a solution-phase method based on seed-mediated growth to produce truncated triangular Ag nanoplates in the presence of micelles assembled from cethyltrimethylammonium(CTAB).[17] In these methods, metal colloidal nanoplates were usually dispersed in liquid phase, which should be separated and rinsed before the some purposes,[18] such as catalysis. Thus, it is still a challenge to find a new way to directly produce Ag nanoplates on the substrate. In addition, construction of some nanostructured devices could also need assembling nanoplates on the substrate directly.

It is well-known that electrochemical deposition can induce growth of nanostructures on the substrate directly. We can kinetically control the growth simply by deposition current density. Different growth process will lead to different morphologies of the products.[19] However, there is very limited report on production of Ag nanoplates with high percentage by electrochemical deposition. Recently, we have synthesized trapeziform silver nanoplates growing on the gold-coated substrate by the electrochemical deposition with proper parameters. The trapeziform Ag nanoplates are standing on the substrate and dispersed uniformly, forming a nanoplate array. This is the first report on such silver nanoplate arrays. Such array could also be a good substrate for SERS if the number density of the standing nanoplates is controlled within a proper range, because edges or corners can serve as "hot site" for the local surface plasmon resonance enhancement.[20]

2. Experimental Section

Silver nitrate ($AgNO_3$, 99+%), and poly(vinyl pyrrolodione) (PVP, MW = 30 000) were purchased from Shanghai Chemical Reagent Co. All chemicals were analytical grade and were used without further purification. Polished silicon (100) wafers were obtained from GRINM Semiconductor Materials Co., Ltd., Beijing. Typically, 1 g/L $AgNO_3$ and 5 g/L PVP were added to 50 mL of water followed by stirring till complete dissolution. Such an aqueous solution was used as the electrolyte in electrodeposition.

A 30−40 nm thick gold layer was sputtered on the polished silicon wafers (2 cm × 0.5 cm). We adopted constant current electrodeposition. A graphite flake was used as anode and the gold-coated silicon (Au/Si) wafer as cathode. The electrochemical deposition was carried out under current density 6 μA/cm^2 for 5 h at room temperature. The Au/Si electrode with products was then taken out, cleaned with distilled water several times, and dried with high-purity flowing nitrogen, before characterization by X-ray diffraction (XRD) (Philips X'pert-PRO, Cu Kα (0.15418nm) radiation), field emission scanning electronic microscope (FESEM, sirion 200 FEG). For transmission electron microscopic (TEM, JEOL 2010, at 200KV) examination, the products were scraped from the Au-coated Si wafer and dispersed in ethanol ultrasonically.

3. Results

3.1. Morphology and Structure. The morphology of the Au/Si electrode without electrodepsoition is shown in Figure 1a. It can be seen that the Au film is composed of small particles with the size of about 40 nm. XRD measurement indicates that such gold film has not preferential orientation (see Figure 1b).

After electrodeposition, FESEM observation shows that the as-prepared products covering the Au/silicon substrate are mainly nanoplates with uniform size and distribution on the substrate, as illustrated in Figure 2. Local magnification has revealed that the sheets are of trapeziform shape with about

* To whom all correspondence should be addressed. E-mail: wpcai@issp.ac.cn.

10.1021/cg700933p CCC: $40.75
Published on Web 07/15/2008

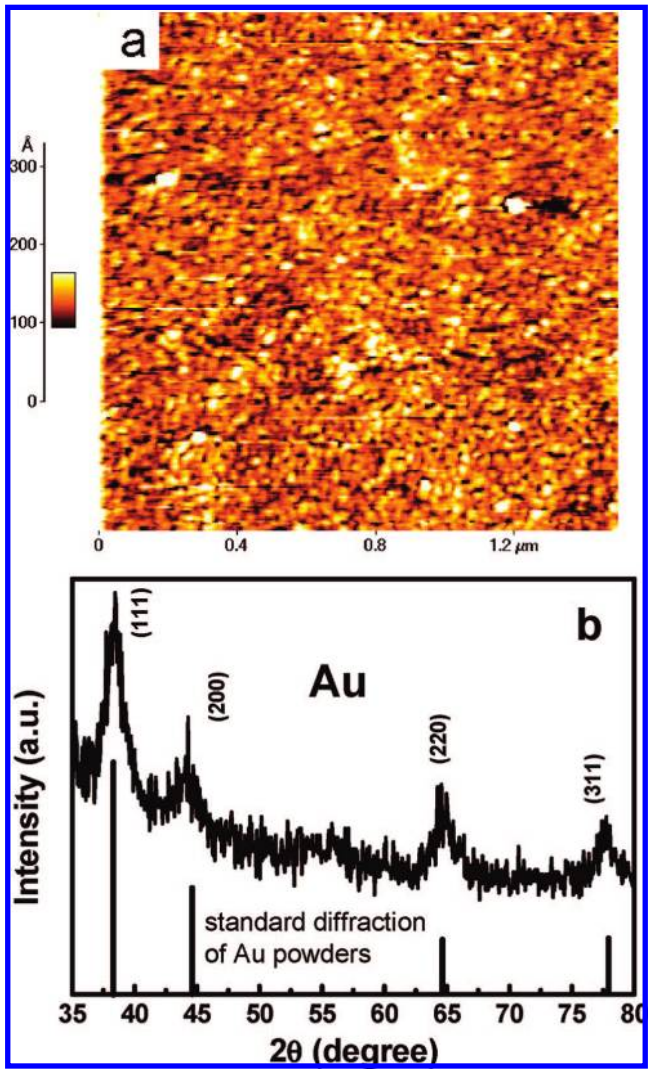

Figure 1. (a) AFM image and (b) XRD of the Au film sputtered on the Si substrate. The lower line spectrum in (b) is the standard diffraction of Au powders.

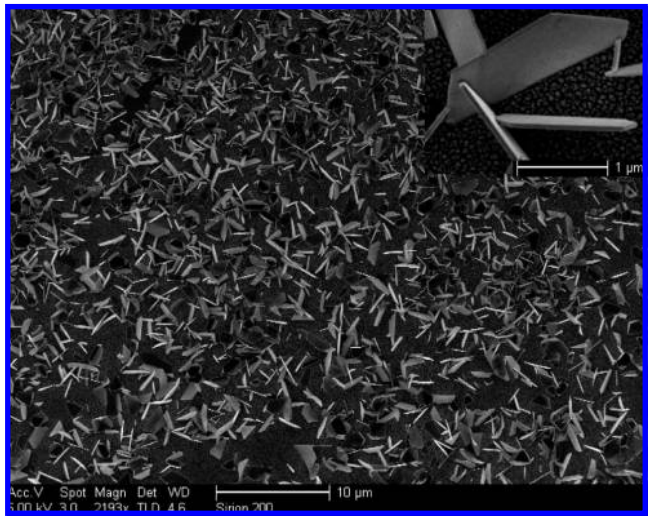

Figure 2. FESEM image of the as-prepared products covering the Au/silicon substrate. Inset: local magnification.

1−2 μm in edge length and 40 nm in thickness, as clearly shown in the inset of Figure 2. It should be mentioned that almost all

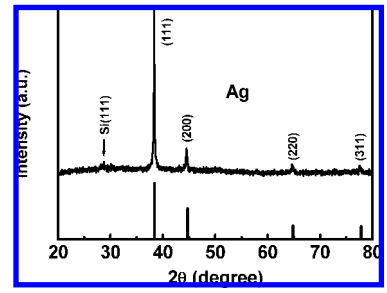

Figure 3. XRD of as-prepared sample shown in Figure 2. The lower line spectrum is the standard diffraction of Ag powders.

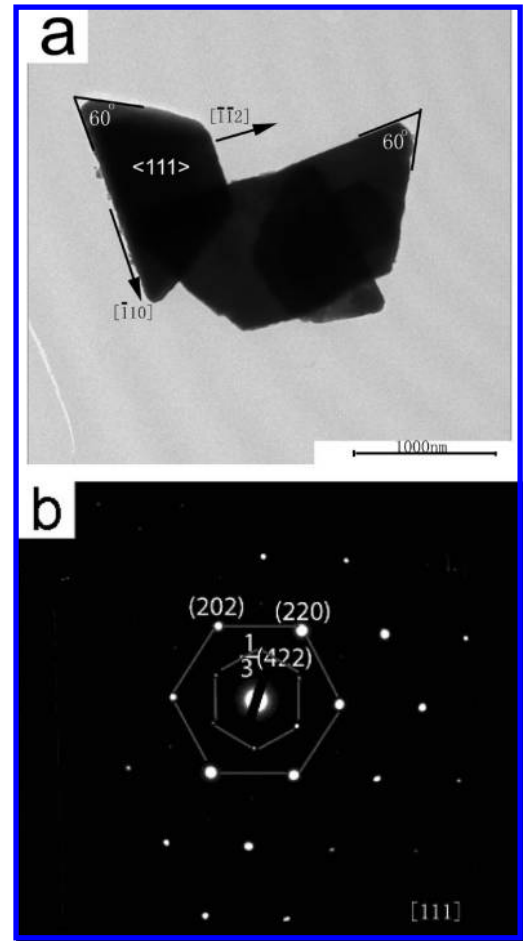

Figure 4. (a) TEM image and (b) corresponding electron diffraction pattern of a single trapeziform Ag nanoplate lying flat on a TEM grid.

the trapeziform Ag nanosheets are standing on the substrate with one side face. The nanosheets strongly adhere to the Au film and can not be removed from the substrate by ultrasonic vibration in water. Figure 3 shows the XRD corresponding to the products shown in Figure 2. All the peaks were indexed to face-centered-cubic (fcc) silver. The intensity ratio of {111} to {200} diffraction peak in the XRD spectrum was about 8, which is much higher than that of bulk Ag (about 2). This indicates that the as-prepared nanoplates are abundant in the {111} planes.

TEM examination shows that the shape of the nanoplate is trapeziform and the angle between adjacent edges is 60 or 120°, as typically shown in Figure 4a corresponding to several trapeziform Ag nanoplates lying on the TEM grid. Figure 4b shows the selected area electron diffraction (SAED) pattern recorded by the electron beam perpendicular to the planar

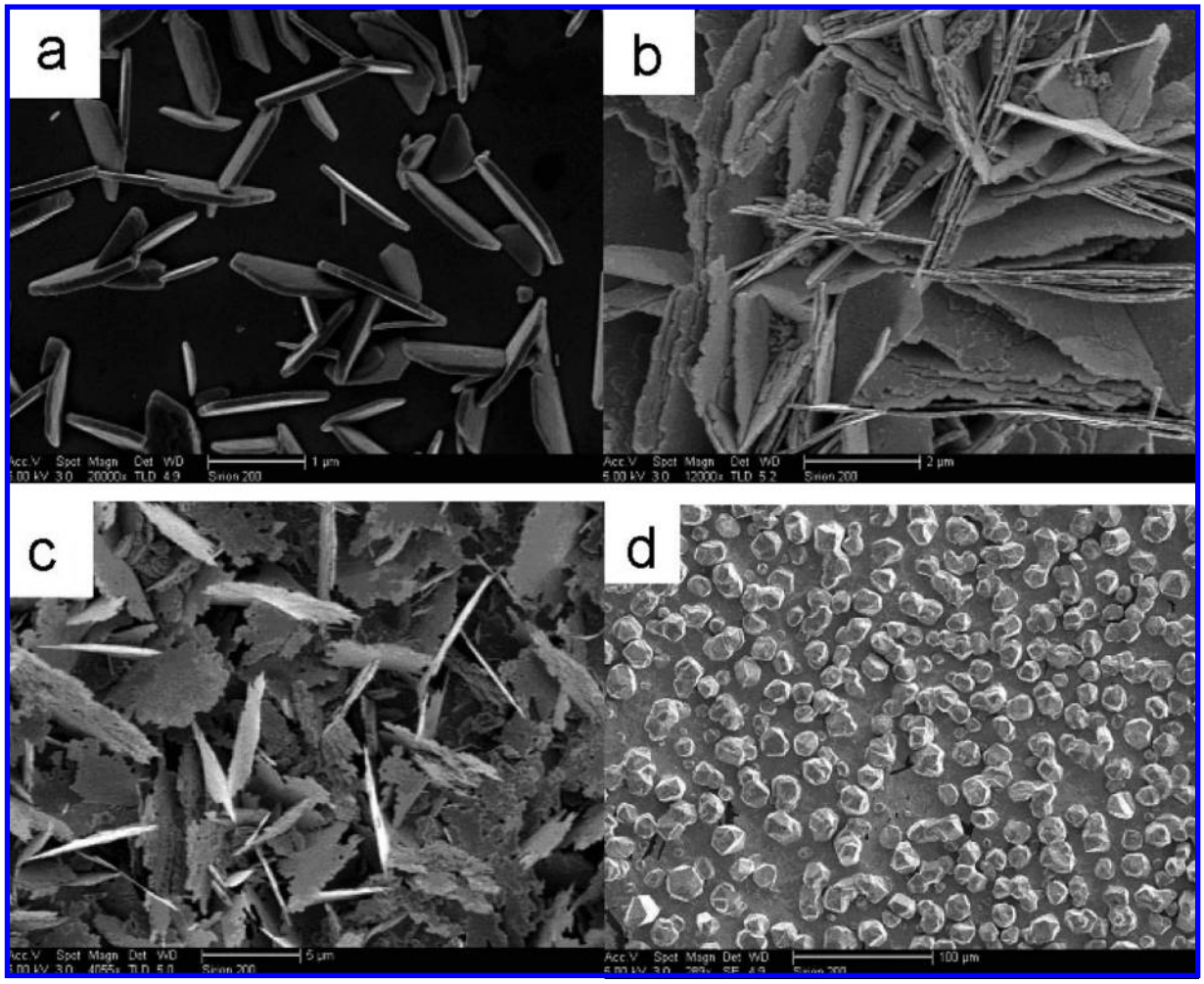

Figure 5. FESEM images of the samples prepared by different deposition current densities (PVP: 5 g/L): (a) 3, (b) 20, (c) 50, and (d) 100 μA/cm^2.

surface of an individual nanoplate lying on the TEM grid. It has revealed that the planar surface of the nanosheets is parallel to the {111}. The inner set of spots in the ⟨111⟩ pattern is believed to originate from the 1/3{422} planes normally forbidden by an fcc lattice. According to the results of Kirkland et al.[21] and Germani et al.,[22] such 1/3 {422} forbidden reflections observed on the plate-like structures of silver or gold should be attributed to {111} stacking faults parallel to the {111} planes and extending across the entire nanoplates. Thus, it is reasonable that two planar surfaces of the standing Ag nanoplates are bound by atomically flat {111} planes. The second set of spots with the strongest intensity is indexed to {220} Bragg reflections, which indicates that the as-prepared nanoplates are single-crystal with {111} lattice planes as the planar surfaces. Also, all the edges should be ⟨110⟩ based on the angles between them. The orientation relationship for the edges and planar surfaces in the nanoplates is marked in Figure 4a.

As for the side walls in the thickness direction of the trapeziform nanoplates (here, we also call "side-surface"), we cannot determine them definitely. On the one hand, from the viewpoint of energy, they may be {100}, which has an angle of about 55° with the planar surface {111}, due to the lower value of surface energy in fcc metals. Although, observed from Figure 2, the most plates are slightly slantwise to the Au substrate, it could be attributed to the surface of Au grains (in the film) which is not definitely parallel to the substrate surface. On the other hand, the side walls are more likely perpendicular to the planar surfaces {111}, observed from the inset of Figure 2 and Figure 4a, than the angle about 55°, although we cannot determine accurate angle between the planar surface and the side-walls. If in this case, the geometric planes (or profile planes) on the side-surfaces should be $\{11\bar{2}\}$. The real surface should be faceted because of its high surface energy, probably with $\{1\bar{1}0\}$, which usually cannot be seen in TEM or FESEM because of the limitation of resolution. Here, we prefer the latter viewpoint, i.e., the side walls are of the profile planes$\{11\bar{2}\}$ and are faceted with $\{1\bar{1}0\}$. Further work is needed. Actually, such side- walls with $\{11\bar{2}\}$ for the Au (or Ag) nanosheets and nanobelts have also been reported.[23,24]

3.2. Influence of Deposition Conditions. Further experiments have revealed that a certain deposition current density is crucial to formation of the trapeziform Ag nanoplates' arrays. In addition, presence of the surfactant PVP is also important for morphologies and sizes of the final products. Figure 5 shows the morphologies of the samples prepared by different deposition current densities keeping the other conditions unchanged. When the current was smaller than 6 μA/cm^2 (say, 3 μA/cm^2), the shape of the particles did not change greatly and still showed trapeziform Ag nanoplates standing on the substrate (see Figure 5a). When the current density is much higher (>15−50 μA/cm^2), the nanosheets are irregularly shaped, as illustrated in images b and c in Figure 5. Furthermore, if the deposition current density is increased to a very high value (say, 100 μA/

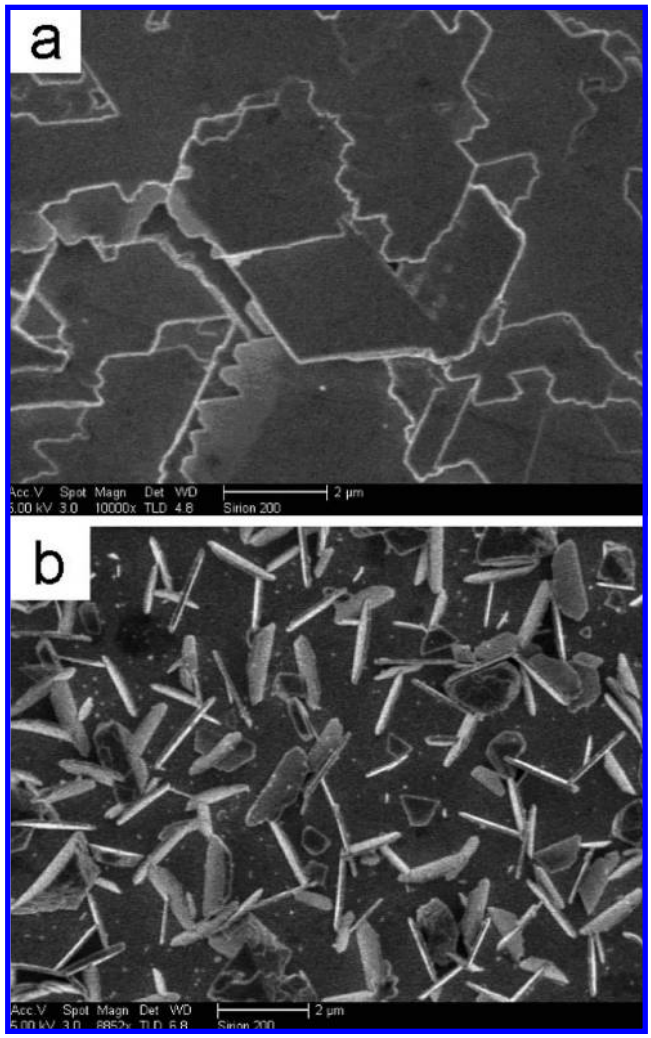

Figure 6. FESEM images of the samples prepared in the electrolyte with (a) 0 and (b) 10 g/L PVP at a deposition current density of 6 μA/cm^2.

cm^2), the final product was dominated by large Ag particles (several to tens of micrometers in size) with equal axial shape. All these indicate that the deposition current density plays a crucial role in the final morphology of the products. Only at a low current density can high-quality trapeziform Ag nanoplates and array be formed.

In addition, if the electrolyte contains no PVP, the silver nanosheets can also be formed at a low electric current density. However, all the nanosheets show irregular outline and are lying, instead of standing, on the substrate, as typically illustrated in Figure 6a. It means that even at absence of PVP Ag nanosheets can still be formed as long as the current density is low enough. At a high concentration of PVP, such as 10 g/L, the products are also trapeziform Ag nanoplates standing on the substrate, as shown in Figure 6b similar to that shown in Figure 2. So, a proper PVP concentration is important to produce high-quality trapeziform Ag nanoplates' array.

Finally, the Au film is crucial for formation of the trapeziform nanoplates' array. If Si substrate without gold coating is used, we cannot get anything on the substrate at a low current density within 5hours. When Au/indium tin oxide (ITO) was used as substrate, we can also get trapeziform Ag nanoplates' array. As for the Ag^+ concentration in the electrolyte, we find only insignificant change in morphology and size of the nanoplates in the range from 0.2 to 5 g/L. It means that the morphology and size of nanoplates are nearly Ag^+ ion concentration-independent.

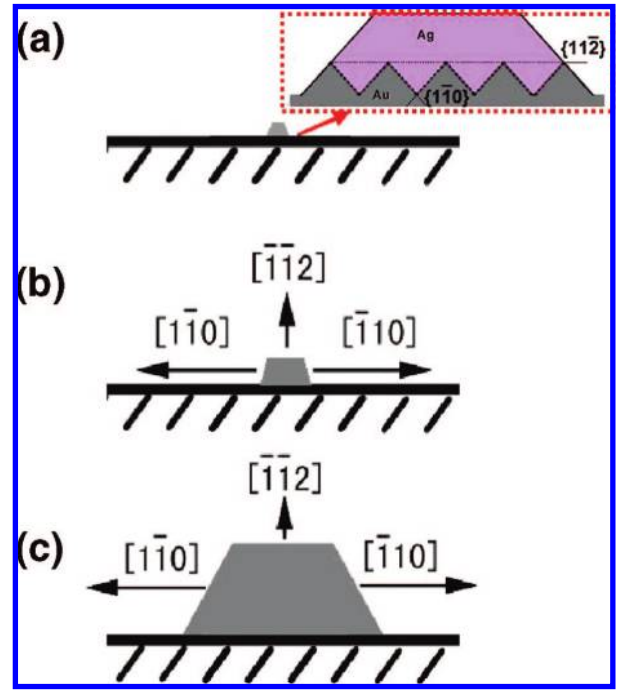

Figure 7. Schematic formation illustration of a trapeziform Ag nanoplate on the Au-coated subatrate. (a) [$\bar{1}\bar{1}$2]-Oriented Ag nucleus on a [$\bar{1}\bar{1}$2]-oriented Au grain with {1$\bar{1}$0} facets in the film ([111] of the Ag nucleus is nearly parallel to the substrate surface); inset: schematic illustration of the magnified area near the interface between the [$\bar{1}\bar{1}$2]-oriented Au grain with {1$\bar{1}$0} facets and the bottom facets of the formed Ag nucleus (the other faceted side-walls are not shown here). (b) Preferential growth of the nuclei along the fastest ⟨110⟩ and secondary fastest [$\bar{1}\bar{1}$2]. (c) Formation of trapeziform nanoplate standing on the substrate.

4. Discussion

4.1. Formation of the Nanoplates. Under the electric field, Ag^+ in the electrolyte will move to surface of the cathode and the reduction reaction take places:

$$Ag^+ + e \rightarrow Ag^o \quad (1)$$

The reduced Ag° atoms will nucleate on the random-oriented Au particles' film. Because PVP in the electrolyte solution will preferentially adsorb on the surface of {111} planes of the Au particles,[25] the nucleation cannot happen on the surface of {111}-oriented Au particles. Here we believe that nucleation takes places preferentially on the nonclosed packing plane or the surface of ⟨11$\bar{2}$⟩-oriented Au nanoparticles in the film due to lower nucleation energy barrier (with higher surface energy) [note: such surface could be faceted with {1$\bar{1}$0}. Also, because of lattice match, the orientation relation Ag ⟨11$\bar{2}$⟩//Au⟨11$\bar{2}$⟩ should exist. At the low electric current density, quasi-equilibrium growth will occur. It means that the formed nuclei grow preferentially along the strong directions ⟨110⟩ within closest packing planes {111}. {111} planes are of the lowest surface energy. The growth along ⟨11$\bar{2}$⟩ is the secondary fastest direction, whereas ⟨111⟩ should be the slowest one under quasi-equilibrium condition. Finally nearly vertically standing trapeziform nanosheets are formed under quasi-equilibrium condition, as schematically shown in Figure 7.

4.2. Influence Factors. On the basis of the discussion above, quasi-equilibrium growth condition (low current density) will

lead to the standing trapeziform nanosheets with high quality. However, if the current density is higher, the growth rate will increase and hence outline of the edges will be rough, leading to irregular shape although there still exists preferential growth or sheetlike growth. When the deposition current density is very high, however, preferential growth will disappear because of the too fast growth rate, inducing nearly isotropic growth and formation of large equal-axial Ag particles (see Figure 5d).

Without PVP in the solution, no adsorption occurs on the Au film. In this case, Ag nuclei could be formed at any site on the film. Sheetlike growth still takes place due to the quasi-equilibrium condition at low current density. Growth of some {111}-oriented Ag nuclei parallel to the substrate will cover the substrate, preventing growth of the other planes-oriented nuclei and leading to no standing nanosheet. Only when PVP is present will selective nucleation occur; the nanosheet array can be formed at a low current density.

As for the substrate with Au coating, selective nucleation can take place, nanoplate array can thus be formed. Also, it is difficult to form a nucleus directly on the Si surface because of the high nucleation energy barrier, leading to no Ag deposition at low current deposition.

5. Conclusion

In summary, trapeziform Ag nanoplate arrays have been successfully synthesized on the Au-coated silicon wafer by a simple and convenient electrochemical deposition at a low current density. The presence of PVP in the electrolyte and low deposition current density together with Au-coated substrate are indispensable to formation of such arrays. Low deposition current can ensure quasi-equilibrium growth and hence formation of Ag nanosheets. Selective adsorption of PVP induces selected and oriented nucleation of Ag, and formation of array standing on the Au film-coated substrate. The preferential growth along $\langle 110 \rangle$ and $\langle 11\bar{2} \rangle$ leads to trapeziform nanoplates. This study is very important for us to vertically immobilize Ag nanoplates on a solid substrate easily. Such nanosheet arrays could be utilized for the substrate of some catalysis or SERS if we get more homogeneous size. The method presented in this paper could also be extended to other metals.

Acknowledgment. This work is financially supported by the National Natural Science Foundation of China (Grants 50671100 and 10604056), the Major State research program of China "Fundamental Investigation on Micro-Nano Sensors and Systems based on BNI Fusion" (Grant 2006CB300402), and the Knowledge Innovation Program of the Chinese Academy of Sciences (Grant KJCX2-SW-W31).

References

(1) Shi, A. C.; Masel, R. I. *J. Catal.* **1989**, *120*, 420.
(2) Chang, S. S.; Shih, C. W.; Chen, C. D.; Lai, W. C.; Wang, C. R. C. *Langmuir* **1999**, *15*, 701.
(3) Pastoriza-Santos, I.; Liz-Marzan, L. M. *Nano Lett.* **2002**, *2*, 903.
(4) (a) Li, C. C.; Cai, W. P.; Cao, B. Q.; Sun, F. S.; Li, Y.; Kan, C. X.; Zhang, L. D. *Adv. Funct. Mater.* **2006**, *16*, 83. (b) Li, C. C.; Shuford, K. L.; Park, Q.-H.; Cai, W. P.; Li, Y.; Lee, C.; Oh, S. *Angew. Chem.,Int. Ed.* **2007**, *119*, 3328.
(5) Kelly, K. L.; Coronado, E.; Zhao, L. L.; Schatz, G. C. *J. Phys. Chem. B* **2003**, *107*, 667.
(6) Peyser, L. A.; Vinson, A. E.; Bartko, A. P.; Dickson, R. M. *Science* **2001**, *291*, 103.
(7) Haes, A. J.; Van Duyne, R. P. *J. Am. Chem. Soc.* **2002**, *124*, 10596.
(8) Sun, S. H.; Murray, C. B.; Weller, D.; Folks, L.; Moser, A. *Science* **2000**, *287*, 1989.
(9) Ahmadi, T. S.; Wang, Z. L.; Green, T. C.; Henglein, A.; El-Sayed, M. A. *Science* **1996**, *272*, 1924.
(10) Fritzsche, W.; Taton, T. A. *Nanotechnology* **2005**, *15*, R63.
(11) Tao, A.; Kim, F.; Hess, C.; Goldberger, J.; He, R. G.; Sun, Y. G.; Xia, Y. N.; Yang, P. D. *Nano Lett.* **2003**, *3*, 1229.
(12) Xiong, Y.; Mclellan, J. M.; Chen, J.; Yin, Y.; Li, Z. Y.; Xia, Y. *J. Am. Chem. Soc.* **2005**, *127*, 17118.
(13) (a) Shankar, S. S.; Rai, A.; Ankamwar, B.; Singh, A.; Ahmad, A.; Sastry, M. *Nat. Mater.* **2004**, *3*, 482. (b) Shankar, S. S.; Rai, A.; Ahmad, A.; Sastry, M. *Chem. Mater.* **2005**, *17*, 566.
(14) Elghanian, R.; Storhoff, J. J.; Mucic, R. C.; Letsinger, R. L.; Mirkin, C. A. *Science* **1997**, *277*, 1078.
(15) Jin, R.; Cao, Y.; Mirkin, C. A.; Kelly, K. L.; Schatz, G. C.; Zheng, J. G. *Science* **2001**, *294*, 1901.
(16) Washio, I.; Xiong, Y. J.; Yin, Y. D.; Xia, Y. N. *Adv. Mater.* **2006**, *18*, 1745.
(17) Chen, S. H.; Fan, Z.; Carroll, D. L. *J. Phys. Chem. B* **2002**, *106*, 10777.
(18) Roucoux, A.; Schulz, J.; Patin, H. *Chem.Rev.* **2002**, *102*, 3757.
(19) Zhou, Y.; Wang, C. Y.; Zhu, Y. R.; Chen, Z. Y. *Chem. Mater.* **1999**, *11*, 2310.
(20) (a) Zhang, J. T.; Li, X. L.; Sun, X. M.; Li, Y. D. *J. Phys. Chem. B* **2005**, *109*, 12544. (b) Duan, G.; Cai, W.; Luo, Y.; Li, Z.; Li, Y. *Appl. Phys. Lett.* **2006**, *89*, 211905.
(21) Kirkland, A. I.; Jefferson, D. A.; Duff, D. G.; Edwards, P. P.; Gameson, I.; Johnson, B. F. G.; Smith, D. *J. Proc. R. Soc. London., Ser. A* **1993**, *440*, 589.
(22) Germani, V.; Li, J.; Ingert, D.; Wang, Z. L.; Pileni, M. P. *J. Phys. Chem. B* **2003**, *107*, 8717.
(23) Aizawa, M.; Cooper, A. M.; Malac, M.; Buriak, J. M. *Nano Lett.* **2005**, *5*, 815.
(24) Zhao, N.; Wei, Y.; Sun, N.; Chen, Q.; Bai, J.; Zhou, L.; Qin, Y.; Li, M.; Qi, L. *Langmuir* **2008**, *24*, 991.
(25) Kan, C. X.; Cai, W. P.; Zhaosing Li, Z. S.; Fu, G. H.; Zhang, L. D. *Chem. Phys. Lett.* **2003**, *382*, 318.

CG700933P